

Structure of an electrorheological fluid in steady shear

James E. Martin and Judy Odinek

Advanced Materials Physics Division, Sandia National Laboratories, Albuquerque, New Mexico 87185

Thomas C. Halsey

The James Franck Institute and Department of Physics, The University of Chicago, 5640 South Ellis Avenue, Chicago, Illinois 60637

(Received 14 January 1994)

We report a real-time, two-dimensional light scattering study of the structure of an electrorheological fluid under steady shear. When an electric field is applied to the quiescent fluid, particles chain along the electric field lines and cause strong light scattering lobes to appear at a finite scattering wave vector q orthogonal to the field lines. We find that when the sample is subjected to steady shear a steady state scattering pattern emerges with lobes that are rotated in the direction of fluid vorticity. The angle of rotation is found to increase as the cube root of the shear rate, in agreement with a theoretical prediction of the steady state structure of fragmenting particle droplets.

PACS number(s): 47.50.+d, 82.70.Dd

Electrorheological (ER) fluids [1,2] are particle suspensions that quickly and reversibly solidify when a strong electric field is applied, due to a mismatch in the dielectric constant or conductivity [3,4] of the particles and the suspending liquid. This mismatch results in induced particle dipoles that cause particle chaining along the electric field lines. When a large shear stress is applied to a soft ER solid, a viscous flow is induced that is strongly shear thinning. Because the viscosity can thus be moderated by the electric field, ER fluids have the potential for applications in electromechanical actuators such as fiber spinning clutches, shock absorbers, etc. In this paper, we report a two-dimensional light scattering study of the structural changes that lead to the shear thinning viscosity in ER fluids at relatively low applied fields.

Experiments [5] show that the viscosity μ of an ER fluid depends inversely on a power of the strain rate $\dot{\gamma}$. The observed exponent increases from $\frac{2}{3}$ at low voltages to 1 at high voltages. The essential cause of shear thinning at low voltages has been described previously [5] in the "independent droplet model." Under the combined influences of shear and an electric field, a column of particles (modeled as an ellipsoidal droplet) will rotate to some angle ϕ relative to the electric field, at which the hydrodynamic and electrostatic torques balance. If the droplet were unable to fragment, ϕ would be proportional to $\dot{\gamma}/E^2$, where the square of the field occurs because the dipoles are induced.

If the hydrodynamic forces cause the droplet to fragment, the remaining shorter pieces will align more closely with the field and ϕ will decrease. In fact, droplets can be observed to break into ever smaller pieces as the shear rate increases, with the result that ϕ increases slowly with shear, specifically as the cube-root law $(\dot{\gamma}/E^2)^{1/3}$. This result for the steady state droplet orientation implies $\mu \propto (\dot{\gamma}/E^2)^{-2/3} \propto \phi^{-2}$ for the shear thinning viscosity. Although ϕ or μ might seem to provide equivalent tests of the independent droplet model, viscosity is such an indirect probe of structure that Stein [6] has quipped "mor-

phology from rheology is theology." In the light scattering measurements reported here, we have determined the shear rate and electric field dependence of the angle ϕ directly. These measurements are a direct determination of the mechanism of the shear thinning, low-field viscosity.

Sample preparation. Light scattering measurements were made on a model colloidal silica fluid, the synthesis of which we have described elsewhere [7]. Briefly, this fluid consists of monodisperse, 0.70- μm silica spheres with a Gaussian sphere radius R distribution of $\sigma_R/R=10.5\%$. The silica spheres are coated with an organophilic silane coupling agent and dispersed in 4-methylcyclohexanol, chosen to closely index match the spheres. The refractive index increment is $dn/dc=0.0017$ ml/g, which is small enough to insure undepolarized single scattering from concentrated dispersions.

The fluid used in this study measured 7.5 wt % by thermal gravimetric analysis. Assuming a silica density of 2.5 g/cm³, this is a volume fraction of 3.0%, which corresponds to a mean separation between sphere centers of $\sim 6R$ and a spacing of $\sim 11R$ between initially formed chains.

The colloids were tested for any electrophoretic mobility due to a residual surface charge both in a Pen Kem Laser Zee microelectrophoresis apparatus and by applying a 1 kV/mm electric field to particles viewed through a Nikon Microphot-FXA optical microscope. No electrophoretic mobility was observed, so there are no direct field interactions.

Apparatus. Our two-dimensional light scattering instrument [7] is based on commonly available video and computer technology. The length scale regime that can be studied is from $2\pi/q=22$ μm to 0.95 μm , where $q=4\pi \sin(\theta/2)/\lambda$ is the scattering wave vector, θ is the scattering angle, and λ is the wavelength in the scattering medium. A 454.5-nm beam from a Coherent argon-ion laser illuminates the shear cell, and the scattered light im-

pinges on a diffusing screen where it is collected by a fixed-gain Pulnix video camera and stored on a VCR tape. For each condition of steady shear, 25 frames of the video signal, with a frame spacing of 1.20 s, are subsequently digitized by a Perceptics PixelBuffer card on a Macintosh Quadra 950 and stored on a 32-Mbyte dual-ported PixelStore memory board. The digitized images have a dynamic range of 256:1 and a spatial resolution of 512×480 .

The images are then checked for stray light due to dust by a simple algorithm that integrates the image intensity and eliminates overly bright images. The intensity is analytically corrected for the incident polarization and incident angle dependent cell, screen reflectances, the emerging angular distribution of light from the diffusing screen, camera vignetting, the Jacobian for light refraction, and the Jacobian of the projection of a sphere onto a flat screen (twice). Although each of these corrections is small, they sum to an intensity correction factor of about 2 at the image edge, relative to the image center. Finally, the images are averaged to reduce noise.

A schematic of the shear cell is shown in Fig. 1. An inner rotating black anodized aluminum electrode of 40.0 mm diameter is surrounded by an outer electrode sandwiched between two black nylatron sheets to create a radial electric field. The electrode gap is 1.0 mm, the electrode width is 2.0 mm, and the entire assembly is "sandwiched" between two glass plates that are separated by 2.0 mm from the sides of the electrodes. This separation improves the uniformity of the shear flow field along the axis of fluid vorticity since the viscous ER fluid is separated from the solid glass surfaces by an essentially

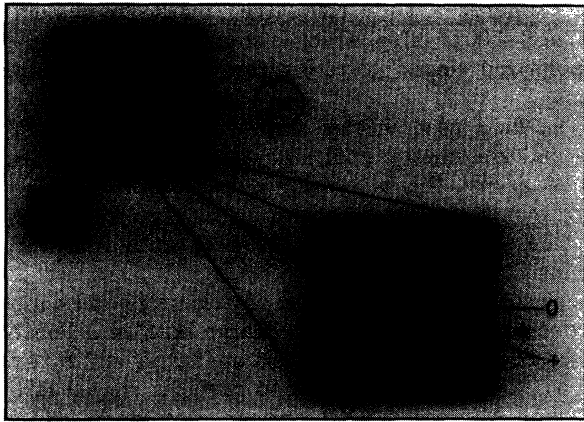


FIG. 1. A schematic of the scattering cell is shown along with the scattering pattern that emerges when a laser beam is directly along the axis of fluid vorticity. The scattering cell consists of an inner, rotating electrode surrounded by an outer electrode that is encapsulated in black nylatron. This assembly is "sandwiched" between glass plates. The electric field is radial and the emerging steady state scattering pattern, which is orthogonal to the electric field for a quiescent fluid, is rotated in the direction of fluid vorticity by some angle ϕ . The maximum intensity occurs at $q=0$, indicating that the quasiperiodicity of column positions in the plane orthogonal to the field, observed in the quiescent fluid, is destroyed.

off-state fluid having a much lower viscosity. The electrode is driven by an NRC rotational stage with a dc servo motor and a precision controller adjustable over 1 decade in speed.

A high slew rate Trek power amplifier, capable of supplying up to 10 kV at 10 mA was used to amplify an unbiased square wave from a WaveTek signal generator. In the voltage and shear rate studies, the frequency was held at 1.0 kHz. Wave form degradation and the appearance of nonohmic conductivity in our sample (usually a sign of incipient dielectric breakdown) limited the applied voltage to 2.5 kV, measured peak to peak.

Measurements. The light scattering behavior of an ER fluid under shear contrasts sharply with that of the quiescent fluid [7]. In the quiescent fluid, structure evolves by chains aggregating into columns, which then aggregate into larger columns *ad infinitum*. Column aggregation is transverse to the electric field, so the phase transition to form a three-dimensional solid occurs in the two-dimensional space orthogonal to the electric field [8]. As a result, an anisotropic light scattering pattern forms with two pronounced lobes orthogonal to the electric field that progressively brighten with time. The maximum intensity in these lobes occurs at a value of $2\pi/q$ corresponding to the mean column separation. This length grows as a power in time and the general scattering behavior is analogous to a two-dimensional system undergoing spinodal decomposition. Eventually an equilibrium solid is formed that has a body-centered tetragonal structure [9,10], provided the colloidal particles are sufficiently monodisperse that a glass is not formed.

When a steady shear is then applied to the sample, the scattering pattern rotates in the direction of fluid vorticity (Fig. 1) and the maximum intensity of the scattering lobes moves to $q=0$. The scattered intensity no longer increases with time, but approaches a steady state value that depends on the shear rate and field. The scattering pattern is consistent with rotated columns whose strong spatial correlations in the direction orthogonal to the column principal axis have been destroyed by shear.

To characterize the scattering data it is necessary to have a systematic method for determining the angle ϕ_{\max} of the rotated scattering data relative to the scattering data of the quiescent fluid, where positive ϕ indicates a rotation in the direction of the fluid vorticity. To determine ϕ_{\max} we first divided a time-averaged scattering image into 360 wedges that each subtend 1° of arc and then determined the scattered intensity in each wedge by integrating the intensity over a preselected q regime that encompasses the scattered signal. We have termed this technique "longitudinal" scattering analysis by analogy to the latitudes and longitudes of the earth; if the laser beam is considered the axis, then we have integrated out the latitudes and are left with the longitudes. Furthermore, the prime meridian is orthogonal to the electric field.

In Fig. 2 we contrast the longitudinal analysis for the quiescent fluid with that of a fluid sheared at 1.06 s^{-1} at an applied voltage of 1.2 kV. The peak maximum is considerably shifted and the half width is much broader than in the quiescent fluid. Operationally, the peak and half

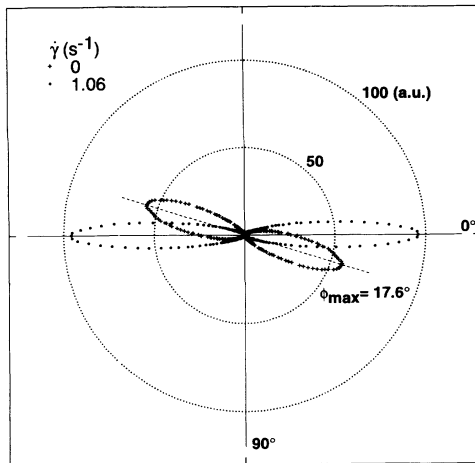


FIG. 2. The integrated intensity of scattered light, obtained from the longitudinal analysis, is shown for an unsheared and sheared sample in the polar coordinates (I, ϕ) . Positive angles are in the direction of fluid vorticity and the small background scattering has been subtracted for clarity. Note that for the sheared sample the scattering pattern is angularly displaced, indicating column tilting. The broadening of the scattering pattern indicates a dispersity of column sizes. The skewing of the scattering pattern is because of the nonlinear dependence of the orientation angle on droplet size. The column orientation can be obtained from a Gaussian fit to the data or from the intensity maximum.

width were extracted from a Gaussian fit to the data, which worked well, despite the fact that the data are slightly skewed. To eliminate the effect of skew in the high shear rate data we also determined the peak position from data close to the maximum.

There are essentially three parameters in this experiment: the applied voltage V , the field frequency ω , and the shear rate $\dot{\gamma}$. Since the magnitude of the ER effect depends on a complex interplay between the frequency dependent conductivities and dielectric constants of the liquid and particulate phases, we felt it prudent to first determine the frequency dependence of the droplet orientation. Over the range of our measurements, which is limited by the slew rate of the power supply, a reasonably flat frequency response was observed (Fig. 3), so we simply selected an intermediate frequency of 1 kHz for our studies. The dependence of the principal column rotation angle ϕ_{\max} on shear rate is shown in Fig. 4. A nonlinear least squares power law fit to the data gives $\phi_{\max} \sim \dot{\gamma}^{0.33}$, in striking agreement with the theoretical prediction of $\phi_{\max} \sim \dot{\gamma}^{1/3}$ from the independent droplet model.

Since the column orientation is due to a balance between the electrostatic and hydrodynamic torques, it is also possible to change the column orientation by keeping the shear rate constant while altering the applied voltage V . The result of this experiment is shown in Fig. 5 for shear rates of 0.34 and 1.40 s^{-1} . At the lowest shear rate a logarithmic plot gives $\phi_{\max} \sim (\dot{\gamma}/V^2)^{0.33}$, in good agreement with the shear rate dependence. However, at a higher shear rate of 1.40 s^{-1} a slight deviation from the expected behavior and a smaller exponent were both observed.

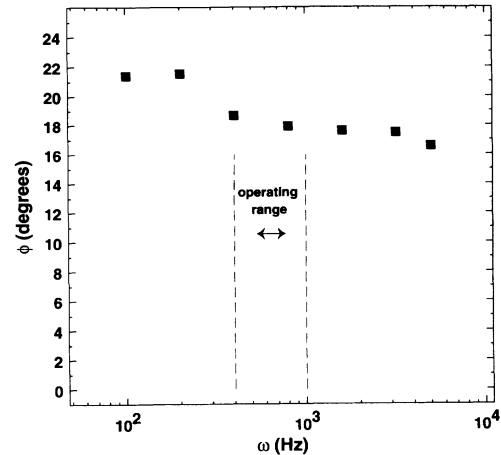


FIG. 3. The dependence of the column orientation angle on the field frequency is shown for a sample at 0.8 kV and a shear rate of 1.4 s^{-1} . The angular displacement is nearly constant in this regime, indicating that the polarizability is nearly frequency independent. Virtually all of our shear and voltage studies were done at 1.0 kHz, although some shear rate studies were done at 400 Hz. Since the particle polarizability is fast and the shear rate is slow, there is no chance of dephasing the particle dipoles by particle rotation.

To gain insight into the nature of the variation we observed, we used a microscope to examine the fluid under shear. A prism or mirror was first placed on the microscope stage to enable viewing in the horizontal direction. A lens was then positioned to image the scattering volume in the shear cell onto the focal plane of the microscope objective, and the unscattered laser beam (attenuated to $\sim 1 \mu\text{W}$) was used as a collimated light source. At

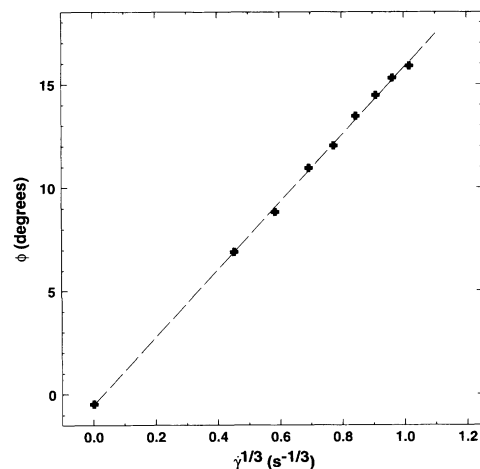


FIG. 4. A plot of the column orientation angle against the cube root of the shear rate shows good linearity, thus bolstering the independent droplet model of structure formation under shear. A nonlinear least squares fit gives $\phi_{\max} \sim \dot{\gamma}^{0.326}$. This particular set of data was taken with an applied frequency of 400 Hz at a peak-to-peak voltage of 1.2 kV.

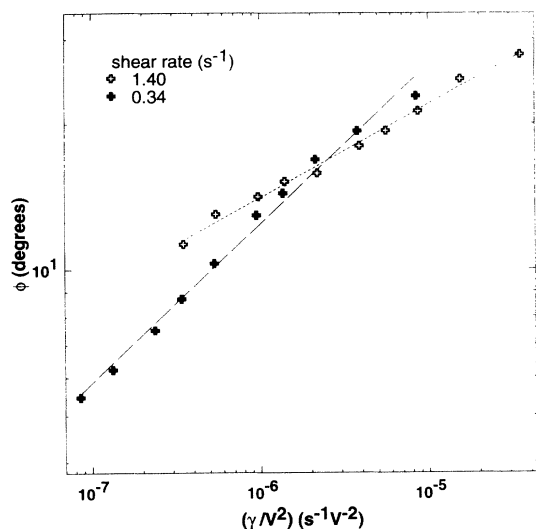


FIG. 5. The orientation angle can be studied as a function of the applied field at constant shear rate. Because the fluid is nonohmic at high voltages, it is expected that the particle and fluid polarizabilities may be field dependent, so the scaling is expected to be somewhat obscured. Still the data at a shear rate of 0.34 s^{-1} are in good agreement with the expected cube-root law.

low voltages, free droplets could be observed in the electrode gap and the orientation of these could be easily changed by altering the voltage or shear rate. However, at high voltages a shear slip zone developed that appeared as columns growing normal to the electrode sur-

face, thus serving to reduce the zone of shear to a regime smaller than the electrode gap. This shear slip zone, which has been previously observed in a different system [11], probably accounts for the observed increase from $\frac{2}{3}$ to 1 in the exponent Δ that describes the shear thinning viscosity through $\mu \sim \dot{\gamma}^{-\Delta}$ as the voltage increases. Of course, since the shear rate in the slip zone is greater than the mean shear rate across the gap, one would expect to observe anomalously large values of the orientation angle, but in reality the situation is more complex since the scattering volume nearly fills the gap.

We have used two-dimensional light scattering to directly determine the structural changes that cause the shear thinning viscosity of ER fluids. Studies of the droplet orientation as a function of the shear rate and the electric field show that the orientation depends on the cube root of the shear rate divided by the field squared. This result is consistent with the independent droplet model of the viscosity. However, at the highest voltages direct microscopy indicates that a shear slip zone occurs with columns growing orthogonally from the electrodes. However, at low particle concentrations and low voltages the mechanism of shear thinning is now understood.

ACKNOWLEDGMENT

J.E.M. and J.O. performed this work at Sandia National Laboratories, Albuquerque, NM, and were supported by the U.S. Department of Energy under Contract No. DE-AC-04-76DP00789. T.C.H. is grateful to the National Science Foundation for the support of this work through Presidential Young Investigator Grant No. DMR-9057156.

- [1] H. Block and J. P. Kelly, *J. Phys. D* **21**, 1661 (1988).
- [2] A. P. Gast and C. F. Zukoski, *Adv. Coll. Inter. Sci.* **30**, 153 (1989).
- [3] R. A. Anderson (unpublished).
- [4] L. C. Davis, *Appl. Phys. Lett.* **60**, 319 (1992).
- [5] T. C. Halsey, J. E. Martin, and D. Adolf, *Phys. Rev. Lett.* **68**, 1519 (1992).
- [6] R. Stein (public communication).
- [7] J. E. Martin, J. Odinek, and T. C. Halsey, *Phys. Rev. Lett.*

- 69**, 1524 (1992).
- [8] T. C. Halsey and W. Toor, *Phys. Rev. Lett.* **65**, 2820 (1990); *J. Stat. Phys.* **61**, 1257 (1990).
- [9] R. Tao and J. M. Sun, *Phys. Rev. Lett.* **67**, 398 (1991).
- [10] T. Chen, R. N. Zitter, and R. Tao, *Phys. Rev. Lett.* **68**, 2555 (1992).
- [11] D. J. Klingenberg and C. Z. Zukoski, *Langmuir* **6**, 15 (1990).

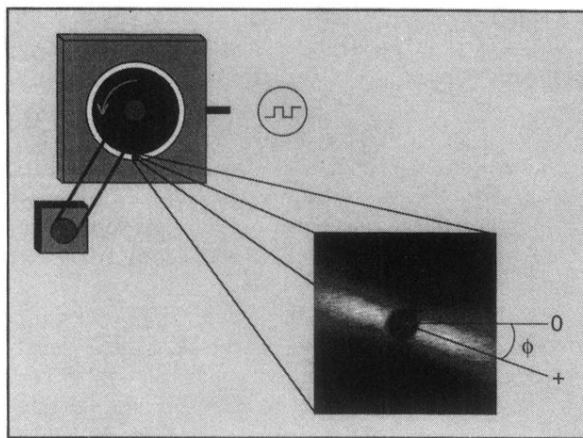


FIG. 1. A schematic of the scattering cell is shown along with the scattering pattern that emerges when a laser beam is directed along the axis of fluid vorticity. The scattering cell consists of an inner, rotating electrode surrounded by an outer electrode that is encapsulated in black nylatron. This assembly is “sandwiched” between glass plates. The electric field is radial and the emerging steady state scattering pattern, which is orthogonal to the electric field for a quiescent fluid, is rotated in the direction of fluid vorticity by some angle ϕ . The maximum intensity occurs at $q=0$, indicating that the quasiperiodicity of column positions in the plane orthogonal to the field, observed in the quiescent fluid, is destroyed.